AIAA JOURNAL
Vol. 50, No. 12, December 2012

Technical Notes

Thrust and Aerodynamic Forces from an Oscillating Leading Edge Flap

Justin W. Jaworski*
University of Cambridge,
Cambridge CB3 0WA, United Kingdom

DOI: 10.2514/1.J051579

Downloaded by MCGILL UNIVERSITY on March 20, 2013 | http://arc.aiaa.org | DOI: 10.2514/1.J051579

Introduction

THIS Note presents in closed form the propulsive force on a rigid, thin airfoil due to sinusoidal actuation of a leading edge flap. The methods of Theodorsen [1] and Garrick [2] are used to arrive at the aerodynamic loads and propulsive efficiency due to harmonic motions of the leading edge flap and its interactions with the traditional plunge, pitching, and trailing edge flap degrees of freedom. These results do not seem to have been published previously and aim to benefit the parameter selection for modern numerical simulations using prescribed leading edge motion to improve period-averaged aerodynamic efficiency [3].

Analysis

Figure 1 illustrates a flat-plate, typical-section airfoil augmented by a leading edge flap with axis location d. The noncirculatory flow potential functions associated with the leading edge flap are determined by integrating over a distribution of source-sink pairs,

$$\phi = \int_{-1}^{d} \frac{\varepsilon}{2\pi} \ell_n \frac{(x-x_1)^2 + (y-y_1)^2}{(x-x_1)^2 + (y+y_1)^2}\, \mathrm{d}x_1 \tag{1}$$

where $y = \sqrt{1-x^2}$. The source strength associated with flap angle ψ is $\varepsilon = \psi U b$, and for angular velocity $\dot{\psi}$ this strength becomes $\varepsilon = \dot{\psi} b^2 (x_1 - d)$. Thus, from Eq. (1) the potential functions for the leading edge flap are

$$\phi_\psi = -\frac{1}{\pi}\psi U b\Big[(c-d)\,\ell_n N + \sqrt{1-x^2}(\pi - \arccos d)\Big] \tag{2}$$

$$\phi_{\dot{\psi}} = \frac{1}{2\pi}\dot{\psi} b^2\Big[\sqrt{1-x^2}\sqrt{1-d^2} - (x-2d)\sqrt{1-x^2} \times (\pi - \arccos d) - (x-d)^2\,\ell_n N\Big] \tag{3}$$

where

$$N = \left|\frac{1 - dx - \sqrt{1-x^2}\sqrt{1-d^2}}{x-d}\right| \tag{4}$$

The noncirculatory lift and moments per unit span follow from direct integration of the potential functions,

$$L_{\mathrm{NC}} = 2\rho b \frac{\partial}{\partial t}\int_{-1}^{1} \phi\, \mathrm{d}x \tag{5}$$

$$(M_\alpha)_{\mathrm{NC}} = -2\rho b^2 \frac{\partial}{\partial t}\int_{-1}^{1} \phi(x-a)\, \mathrm{d}x + 2\rho U b \int_{-1}^{1} \phi\, \mathrm{d}x \tag{6}$$

$$(M_\beta)_{\mathrm{NC}} = -2\rho b^2 \frac{\partial}{\partial t}\int_{c}^{1} \phi(x-c)\, \mathrm{d}x + 2\rho U b \int_{c}^{1} \phi\, \mathrm{d}x \tag{7}$$

$$(M_\psi)_{\mathrm{NC}} = -2\rho b^2 \frac{\partial}{\partial t}\int_{-1}^{d} \phi(x-d)\, \mathrm{d}x + 2\rho U b \int_{-1}^{d} \phi\, \mathrm{d}x \tag{8}$$

where ρ is the fluid density, U is the freestream velocity, and b is the semi-chord length. The aerodynamic moments on the total airfoil, trailing edge flap alone, and leading edge flap alone are calculated about axis locations a, c, and d, respectively. Note that ϕ in Eqs. (5–8) represents the sum of the leading edge velocity potentials and the potentials due to pitching, plunge, and the trailing edge motions outlined by Theodorsen [1].

The relationships between the noncirculatory loads and the total aerodynamic loads for sinusoidal motions are well-known [4], and here we note the new result for the moment about the elastic axis of the leading edge flap.[†]

$$M_\psi = (M_\psi)_{\mathrm{NC}} - \rho U b^2 Q\{Z_1 - Z_{15}C\} \tag{9}$$

where $C = C(k) = H_1^{(2)}(k)/[H_1^{(2)}(k) + iH_0^{(2)}(k)] = F + iG$ is understood to be the classical Theodorsen function [1] of the reduced frequency, $k = \omega b/U$. The Kutta condition sets the magnitude of the circulation from the downwash profile of the airfoil, which defines Q in the usual fashion as

$$Q = U\alpha + \dot{h} + b\left(\frac{1}{2} - a\right)\dot{\alpha} + \frac{T_{10}}{\pi}U\beta + \frac{T_{11}}{2\pi}b\dot{\beta} + \frac{Z_{13}}{\pi}U\psi + \frac{Z_{14}}{2\pi}b\dot{\psi} \tag{10}$$

Lift and Moments

The total lift and moments can now be written as a linear superposition of Theodorsen's results [1] with the new contributions of the leading edge flap. Agreement with Kerschen [5] is noted for the unsteady lift due to the leading edge flap.

$$L = \pi\rho b^2\left[U\dot{\alpha} + \ddot{h} - ba\ddot{\alpha} - \frac{T_4}{\pi}U\dot{\beta} - \frac{T_1}{\pi}b\ddot{\beta} - \frac{Z_1}{\pi}U\dot{\psi} + \frac{Z_2}{\pi}b\ddot{\psi}\right] + 2\pi\rho U b C Q \tag{11}$$

$$M_\alpha = -\pi\rho b^2\left[\left(\frac{1}{2} - a\right)Ub\dot{\alpha} + b^2\left(\frac{1}{8} + a^2\right)\ddot{\alpha} - ba\ddot{h} + \frac{T_{15}}{\pi}U^2\beta + \frac{T_{16}}{\pi}Ub\dot{\beta} + \frac{2T_{13}}{\pi}b^2\ddot{\beta} + \frac{Z_{16}}{\pi}U^2\psi + \frac{Z_{17}}{\pi}Ub\dot{\psi} + \frac{Z_4}{\pi}b^2\ddot{\psi}\right] + 2\pi\rho U b^2\left(a + \frac{1}{2}\right)CQ \tag{12}$$

$$M_\beta = -\rho b^2\left\{T_{17}Ub\dot{\alpha} + 2T_{13}b^2\ddot{\alpha} - T_1 b\ddot{h} + \frac{T_{18}}{\pi}U^2\beta - \frac{T_{19}}{2\pi}Ub\dot{\beta} - \frac{T_3}{\pi}b^2\ddot{\beta} - \frac{Z_{18}}{\pi}U^2\psi - \frac{Z_{19}}{\pi}Ub\dot{\psi} + \frac{Z_{12}}{\pi}b^2\ddot{\psi}\right\} - \rho U b^2 T_{12} C Q \tag{13}$$

Received 26 August 2011; revision received 1 April 2012; accepted for publication 2 April 2012. Copyright © 2012 by Justin W. Jaworski. Published by the American Institute of Aeronautics and Astronautics, Inc., with permission. Copies of this paper may be made for personal or internal use, on condition that the copier pay the $10.00 per-copy fee to the Copyright Clearance Center, Inc., 222 Rosewood Drive, Danvers, MA 01923; include the code 0001-1452/12 and $10.00 in correspondence with the CCC.

*NSF Research Fellow, Department of Applied Mathematics and Theoretical Physics. Member AIAA.

[†]Constants resulting from various integrations are tabulated in the appendix.

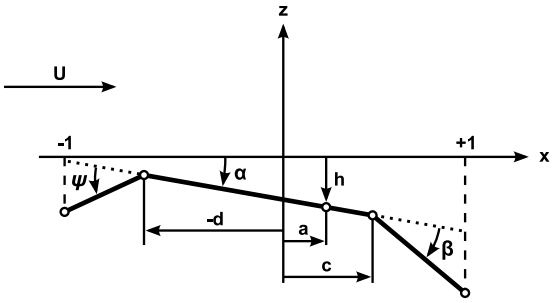

Fig. 1 Schematic of flat plate airfoil with flaps at the leading and trailing edges.

$$M_\psi = \rho b^2 \left\{ Z_{20} U b \dot{\alpha} + Z_4 b^2 \ddot{\alpha} + Z_2 b \ddot{h} - \frac{Z_{21}}{\pi} U^2 \beta + \frac{Z_{22}}{\pi} U b \dot{\beta} + \frac{Z_{12}}{\pi} b^2 \ddot{\beta} - \frac{Z_{23}}{\pi} U^2 \psi - \frac{Z_{24}}{2\pi} U b \dot{\psi} + \frac{Z_8}{\pi} b^2 \ddot{\psi} \right\} + \rho U b^2 Z_{15} C Q \tag{14}$$

Thrust

Consider the following harmonic airfoil motions,

$$\alpha = \alpha_0 e^{i(\omega t + \theta_0)} \tag{15}$$

$$\beta = \beta_0 e^{i(\omega t + \theta_1)} \tag{16}$$

$$h = h_0 e^{i(\omega t + \theta_2)} \tag{17}$$

$$\psi = \psi_0 e^{i(\omega t + \theta_3)} \tag{18}$$

The method of von Kármán and Burgers [6] and Garrick [2] is employed to determine the average propulsive force over a period of prescribed motion by the following energy balance.

$$\bar{W} = \bar{E} + \bar{P}_x U \tag{19}$$

In words, the average power to maintain the prescribed motions of the airfoil against the aerodynamic forces and moments, $\bar{W}$, is equal to the average increase in energy shed into the wake in unit time, $\bar{E}$, the average work done in unit time by the propulsive force P_x [2]. The instantaneous work required to maintain the oscillations is

$$\dot{W} = -(-L\dot{h} + M_\alpha \dot{\alpha} + M_\beta \dot{\beta} - M_\psi \dot{\psi}) \tag{20}$$

Thus, the average power per period of prescribed motion to sustain the airfoil motions is

$$\bar{W} = \frac{\omega}{2\pi} \int_0^{2\pi/\omega} \dot{W} \, \mathrm{d}t \tag{21}$$

$$= \pi \rho b^2 \frac{\omega^3}{k} (B_1 h_0^2 + B_2 \alpha_0^2 + B_3 \beta_0^2 + B_4 \psi_0^2 + 2B_5 \alpha_0 h_0 + 2B_6 \beta_0 h_0 + 2B_7 \psi_0 h_0 + 2B_8 \alpha_0 \beta_0 + 2B_9 \alpha_0 \psi_0 + 2B_{10} \beta_0 \psi_0) \tag{22}$$

Garrick [2] showed that if one decomposes $Qe^{-i\omega t}$ into $A + iB$, the average value of the increase in energy in the fluid in unit time may be expressed as

$$\bar{E} = \frac{2\rho U b}{kD} (A^2 + B^2) \tag{23}$$

$$= \pi \rho b^2 \frac{\omega^3}{k} (C_1 h_0^2 + C_2 \alpha_0^2 + C_3 \beta_0^2 + C_4 \psi_0^2 + 2C_5 \alpha_0 h_0 + 2C_6 \beta_0 h_0 + 2C_7 \psi_0 h_0 + 2C_8 \alpha_0 \beta_0 + 2C_9 \alpha_0 \psi_0 + 2C_{10} \beta_0 \psi_0) \tag{24}$$

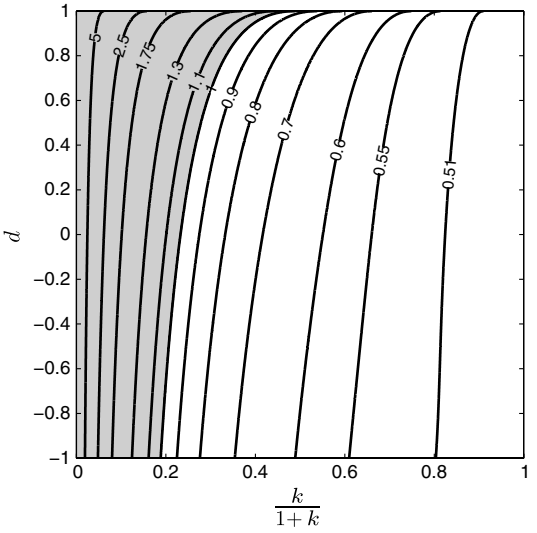

Fig. 2 Contours of $\bar{E}/\bar{W} = 1 - \eta_p$ for an oscillating leading edge flap. The shaded region indicates period-averaged drag.

The efficiency of the thrust production follows from a rearrangement of Eq. (19),

$$\eta_p \equiv \frac{\bar{P}_x U}{\bar{W}} = 1 - \frac{\bar{E}}{\bar{W}} \tag{25}$$

which enables the calculation of propulsive efficiency from the coefficients in Eqs. (22) and (24) tabulated in the appendix.

Consider the special case of an isolated leading edge flap (h_0, α_0, $\beta_0 = 0$) oscillating about pitch axis d. Figure 2 plots contours of $\bar{E}/\bar{W}$ over the complete range of reduced frequency and axis locations of the flap. Values less than unity denote propulsion, whereas values greater than unity indicate drag. The result by Garrick [2] for an airfoil pitching at the trailing edge is recovered as $d \to 1$, where thrust is achieved for reduced frequencies above $k = 0.9577$, or $k^* \equiv k/(1+k) = 0.4892$.

Figure 3 compares this critical frequency of an oscillating leading edge flap against that of a trailing edge flap as a function of axis location. Recall that the axis location is d for the leading edge flap and c for the trailing edge flap. The trailing edge flap must generally comprise a substantial portion of the airfoil chord to achieve thrust, and the minimum critical frequency for the trailing edge flap is $k = 0.6336$ ($k^* = 0.3879$) as $c \to -1$. As the trailing edge flap becomes infinitely small ($c \to 1$), there does not exist a finite frequency above which thrust can be produced, i.e. $k^* \to 1$ or $k \to \infty$.

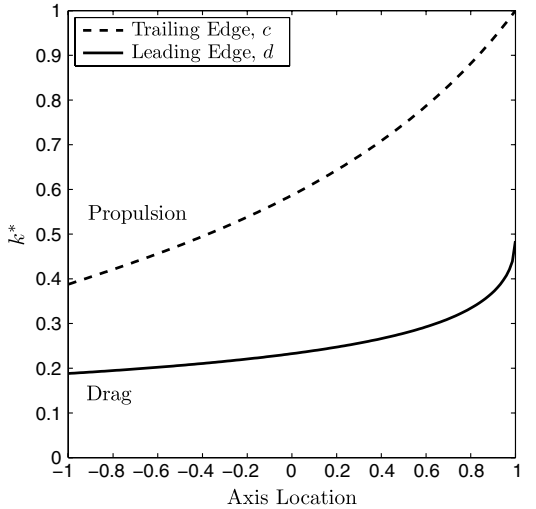

Fig. 3 Critical frequency to produce thrust from an oscillating leading or trailing edge flap as a function of axis location.

Downloaded by MCGILL UNIVERSITY on March 20, 2013 | http://arc.aiaa.org | DOI: 10.2514/1.J051579

A surprising result of mathematical interest is noted for the case of an oscillating leading edge flap of infinitesimal extent. In the formal limit as $d \to -1$, thrust is still produced above a critical frequency $k = 0.2319$ ($k^* = 0.1883$), which is also the minimum frequency to achieve propulsion with harmonic leading-edge actuation. Thus, Figs. 2 and 3 also suggest that oscillating leading edge flaps occupying a smaller fraction of the chord length are more efficient propulsors at low frequency. However, the practical point should be made that propulsive efficiency depends on the ratio $\bar{E}/\bar{W}$, whereas the magnitude of the propulsive force varies with the algebraic difference $\bar{W} - \bar{E}$. This distinction can allow an oscillating trailing edge flap to produce a thrust greater in magnitude than a leading edge flap with the same unsteady amplitude and length per unit chord. Indeed, the capacity to attain a greater propulsive force is an important concern for airfoils oscillating in real fluids, where a sufficiently large force is necessary to overcome the drag associated with viscous stresses in order to achieve a net thrust [7].

Conclusion

The classical analysis for the aerodynamic loads on an oscillating airfoil is extended to include the additional degree of freedom of a leading edge flap and its interaction with the standard plunge, pitch, and trailing edge flap motions. It is shown in the special case of an isolated leading edge flap that there exists for every hinge location a finite frequency to achieve a net thrust on the airfoil. Also, the minimum frequency to achieve a net thrust occurs for a leading edge flap of infinitesimal extent, in contrast to an oscillating trailing edge flap which achieves propulsion at lower frequencies when its length is maximized.

Appendix

The coefficients denoted by T are tabulated in full by Garrick [2]. New coefficients based on the present analysis are denoted by Z.

$$Z_1 = d\sqrt{1-d^2} + (\pi - \arccos d) \tag{A1}$$

$$Z_2 = \frac{1}{3}(2+d^2)\sqrt{1-d^2} + d(\pi - \arccos d) \tag{A2}$$

$$Z_3 = \frac{1}{3}(1-d^2)^{3/2} + a\left[(\pi - \arccos d) + d\sqrt{1-d^2}\right] \tag{A3}$$

$$Z_4 = \frac{1}{24}\sqrt{1-d^2}\left[d(2d^2-5) - 8a(2+d^2)\right] - (\pi - \arccos d)\left(\frac{1}{8} + ad\right) \tag{A4}$$

$$Z_5 = (1-d^2) + 2d\sqrt{1-d^2}(\pi - \arccos d) + (\pi - \arccos d)^2 \tag{A5}$$

$$Z_6 = d(1-d^2) + (1+d^2)\sqrt{1-d^2}(\pi - \arccos d) + d(\pi - \arccos d)^2 \tag{A6}$$

$$Z_7 = Z_6 \tag{A7}$$

$$Z_8 = \frac{1}{8}(1-d^2)(4+5d^2) + \frac{1}{4}d\sqrt{1-d^2}(7+2d^2)(\pi - \arccos d) + \left(\frac{1}{8} + d^2\right)(\pi - \arccos d)^2 \tag{A8}$$

$$Z_9 = (c-d)^2 \ln N_{cd} - \sqrt{1-d^2}(-\sqrt{1-c^2} + d\arccos c) + (\pi - \arccos d)(c\sqrt{1-c^2} - \arccos c) \tag{A9}$$

$$Z_{10} = \frac{1}{3}(c-d)^3 \ln N_{cd} + \frac{1}{3}\sqrt{1-d^2}\left[-(c+2d)\sqrt{1-c^2} + (2+d^2)\arccos c\right] + (\pi - \arccos d) \times \left[\frac{1}{3}\sqrt{1-c^2}(c^2 - 3cd - 1) + d\arccos c\right] \tag{A10}$$

$$Z_{11} = \frac{1}{3}(c-d)^3 \ln N_{cd} + \frac{1}{3}\sqrt{1-d^2}\left[\sqrt{1-c^2}(2c+d) + (d^2 - 3cd - 1)\arccos c\right] + (\pi - \arccos d) \times \left[\frac{1}{3}\sqrt{1-c^2}(2+c^2) - c\arccos c\right] \tag{A11}$$

$$Z_{12} = \frac{1}{24}[8d(c^2+2) - c(2c^2-5)]\sqrt{1-c^2}(\pi - \arccos d) - \frac{1}{24}[8c(d^2+2) - d(2d^2-5)]\sqrt{1-d^2}\arccos c + \frac{1}{24}[c(2c+11d) + 2(d^2+6)]\sqrt{1-c^2}\sqrt{1-d^2} - \left(\frac{1}{8} + cd\right)(\pi - \arccos d)\arccos c - \frac{1}{12}(c-d)^4 \ln N_{cd} \tag{A12}$$

$$Z_{13} = \sqrt{1-d^2} - (\pi - \arccos d) \tag{A13}$$

$$Z_{14} = (2d-1)(\pi - \arccos d) + (2-d)\sqrt{1-d^2} \tag{A14}$$

$$Z_{15} = (\pi - \arccos d)(2d+1) + (d+2)\sqrt{1-d^2} \tag{A15}$$

$$Z_{16} = Z_1 + Z_{13} \tag{A16}$$

$$Z_{17} = -Z_2 + Z_3 + \frac{1}{2}Z_{14} \tag{A17}$$

$$Z_{18} = Z_9 + T_4 Z_{13} \tag{A18}$$

$$Z_{19} = Z_{10} + Z_{11} + \frac{1}{2}T_4 Z_{14} \tag{A19}$$

$$Z_{20} = Z_2 - Z_3 - \left(\frac{1}{2} - a\right)Z_1 \tag{A20}$$

$$Z_{21} = Z_9 + T_{10} Z_1 \tag{A21}$$

$$Z_{22} = Z_{10} + Z_{11} - T_{11} Z_1 \tag{A22}$$

$$Z_{23} = Z_5 + Z_1 Z_{13} \tag{A23}$$

$$Z_{24} = Z_1 Z_{14} \tag{A24}$$

$$N_{cd} = \left|\frac{1 - cd - \sqrt{1-c^2}\sqrt{1-d^2}}{c-d}\right| \tag{A25}$$

Coefficients related to the calculation of $\bar{E}$ and $\bar{W}$ are presented below, which confirm and augment the analysis of Garrick [2] with new results B_4, B_8, B_9, B_{10}, C_4, C_8, C_9, and C_{10}.

$$B_1 = F \tag{A26}$$

Downloaded by MCGILL UNIVERSITY on March 20, 2013 | http://arc.aiaa.org | DOI: 10.2514/1.J051579

$$B_2 = b^2\left\{\frac{1}{2}\left(\frac{1}{2}-a\right)-\left(a+\frac{1}{2}\right)\left[F\left(\frac{1}{2}-a\right)+\frac{G}{k}\right]\right\} \tag{A27}$$

$$B_3 = b^2\left\{-\frac{T_{19}}{4\pi^2}+\frac{T_{12}}{2\pi}\left[\frac{T_{11}}{2\pi}F+\frac{T_{10}}{\pi}\frac{G}{k}\right]\right\} \tag{A28}$$

$$B_4 = b^2\left\{-\frac{Z_{24}}{4\pi^2}+\frac{Z_{15}}{2\pi}\left[\frac{Z_{14}}{2\pi}F+\frac{Z_{13}}{\pi}\frac{G}{k}\right]\right\} \tag{A29}$$

$$B_5 = \frac{b}{2}\left\{\left[\frac{1}{2}-2aF+\frac{G}{k}\right]\cos(\theta_2-\theta_0)-\left[\frac{F}{k}-G\right]\sin(\theta_2-\theta_0)\right\} \tag{A30}$$

$$B_6 = \frac{b}{2}\left\{\left[-\frac{T_4}{2\pi}+\frac{T_{11}+T_{12}}{2\pi}F+\frac{T_{10}}{\pi}\frac{G}{k}\right]\cos(\theta_2-\theta_1) - \left[\frac{T_{10}}{\pi}\frac{F}{k}+\frac{T_4}{\pi}G\right]\sin(\theta_2-\theta_1)\right\} \tag{A31}$$

$$B_7 = \frac{b}{2}\left\{\left[-\frac{Z_1}{2\pi}+\frac{Z_{14}+Z_{15}}{2\pi}F+\frac{Z_{13}}{\pi}\frac{G}{k}\right]\cos(\theta_3-\theta_2) + \left[\frac{Z_{13}}{\pi}\frac{F}{k}+\frac{Z_1}{\pi}G\right]\sin(\theta_3-\theta_2)\right\} \tag{A32}$$

$$B_8 = \frac{b^2}{2}\left\{\left[\frac{T_{11}}{4\pi}-\left(\frac{1}{2}-a\right)\frac{T_4}{2\pi}+\left(\frac{T_4}{2\pi}-\frac{T_{11}+T_{12}}{2\pi}a\right)F - \left(\frac{T_{10}}{\pi}\left(a+\frac{1}{2}\right)-\frac{T_{12}}{2\pi}\right)\frac{G}{k}\right]\cos(\theta_1-\theta_0) + \left[\frac{T_{15}}{2\pi}\frac{1}{k}-\left(\frac{T_{10}}{\pi}\left(a+\frac{1}{2}\right)+\frac{T_{12}}{2\pi}\right)\frac{F}{k} + \left(\frac{T_{11}+T_{12}}{4\pi}-\frac{T_4}{\pi}a\right)G\right]\sin(\theta_1-\theta_0)\right\} \tag{A33}$$

$$B_9 = \frac{b^2}{2}\left\{\left[\frac{Z_{14}}{4\pi}-\left(\frac{1}{2}-a\right)\frac{Z_1}{2\pi}+\left(\frac{Z_1}{2\pi}-\frac{Z_{14}+Z_{15}}{2\pi}a\right)F - \left(\frac{Z_{13}}{\pi}\left(a+\frac{1}{2}\right)-\frac{Z_{15}}{2\pi}\right)\frac{G}{k}\right]\cos(\theta_3-\theta_0) + \left[\frac{Z_{16}}{2\pi}\frac{1}{k}-\left(\frac{Z_{13}}{\pi}\left(a+\frac{1}{2}\right)+\frac{Z_{15}}{2\pi}\right)\frac{F}{k} + \left(\frac{Z_{14}+Z_{15}}{4\pi}-\frac{Z_1}{\pi}a\right)G\right]\sin(\theta_3-\theta_0)\right\} \tag{A34}$$

$$B_{10} = \frac{b^2}{2}\left\{\left[-\frac{T_{11}Z_1}{2\pi^2}-\frac{T_4Z_{14}}{4\pi^2}+\frac{T_{11}Z_{15}+T_{12}Z_{14}}{4\pi^2}F + \frac{T_{10}Z_{15}+T_{12}Z_{13}}{2\pi^2}\frac{G}{k}\right]\cos(\theta_3-\theta_1)-\left[\frac{T_4Z_{13}-T_{10}Z_1}{2\pi^2}\frac{1}{k} + \frac{T_{10}Z_{15}-T_{12}Z_{13}}{2\pi^2}\frac{F}{k}-\frac{T_{11}Z_{15}-T_{12}Z_{14}}{4\pi^2}G\right]\sin(\theta_3-\theta_1)\right\} \tag{A35}$$

$$C_1 = \frac{2}{\pi kD} \tag{A36}$$

$$C_2 = \frac{2b^2}{\pi kD}\left[\frac{1}{k^2}+\left(\frac{1}{2}-a\right)^2\right] \tag{A37}$$

$$C_3 = \frac{2b^2}{\pi kD}\left[\left(\frac{T_{10}}{\pi k}\right)^2+\left(\frac{T_{11}}{2\pi}\right)^2\right] \tag{A38}$$

$$C_4 = \frac{2b^2}{\pi kD}\left[\left(\frac{Z_{13}}{\pi k}\right)^2+\left(\frac{Z_{14}}{2\pi}\right)^2\right] \tag{A39}$$

$$C_5 = \frac{2b}{\pi kD}\left[\left(\frac{1}{2}-a\right)\cos(\theta_2-\theta_0)-\frac{1}{k}\sin(\theta_2-\theta_0)\right] \tag{A40}$$

$$C_6 = \frac{2b}{\pi kD}\left[\frac{T_{11}}{2\pi}\cos(\theta_2-\theta_1)-\frac{T_{10}}{\pi k}\sin(\theta_2-\theta_1)\right] \tag{A41}$$

$$C_7 = \frac{2b}{\pi kD}\left[\frac{Z_{14}}{2\pi}\cos(\theta_3-\theta_2)+\frac{Z_{13}}{\pi k}\sin(\theta_3-\theta_2)\right] \tag{A42}$$

$$C_8 = \frac{2b^2}{\pi kD}\left\{\left[\frac{T_{10}}{\pi k^2}+\left(\frac{1}{2}-a\right)\frac{T_{11}}{2\pi}\right]\cos(\theta_1-\theta_0) + \frac{1}{k}\left[\frac{T_{10}}{\pi}\left(\frac{1}{2}-a\right)-\frac{T_{11}}{2\pi}\right]\sin(\theta_1-\theta_0)\right\} \tag{A43}$$

$$C_9 = \frac{2b^2}{\pi kD}\left\{\left[\frac{Z_{13}}{\pi k^2}+\left(\frac{1}{2}-a\right)\frac{Z_{14}}{2\pi}\right]\cos(\theta_3-\theta_0) + \frac{1}{k}\left[\frac{Z_{13}}{\pi}\left(\frac{1}{2}-a\right)-\frac{Z_{14}}{2\pi}\right]\sin(\theta_3-\theta_0)\right\} \tag{A44}$$

$$C_{10} = \frac{2b^2}{\pi kD}\left\{\left[\frac{T_{10}Z_{13}}{\pi^2k^2}+\frac{T_{11}Z_{14}}{4\pi^2}\right]\cos(\theta_3-\theta_1) + \left[\frac{T_{11}Z_{13}-T_{10}Z_{14}}{2\pi^2k}\right]\sin(\theta_3-\theta_1)\right\} \tag{A45}$$

where

$$D = D(k) \equiv [J_1(k)+Y_0(k)]^2+[Y_1(k)-J_0(k)]^2 \tag{A46}$$

Acknowledgments

This work was supported in part by a National Research Council Research Associateship Award held at Wright-Patterson AFB, USA and by the National Science Foundation under Award No. 0965248. The insightful comments by the anonymous reviewers are gratefully acknowledged.

References

[1] Theodorsen, T., "General Theory of Aerodynamic Instability and the Mechanism of Flutter," NACA, Technical Rept. TR 496, 1935.

[2] Garrick, I. E., "Propulsion of a Flapping and Oscillating Airfoil," NACA, Technical Rept. TR 567, 1936.

[3] Drost, K. J., Johnson, H., Apte, S. V., and Liburdy, J. A., "Low Reynolds Number Flow Dynamics of a Thin Airfoil with an Actuated Leading Edge," *41st AIAA Fluid Dynamics Conference and Exhibit*, AIAA Paper 2011-3904, Honolulu, HI, June 2011.

[4] Bisplinghoff, R. L., Ashley, H., and Halfman, R. L., *Aeroelasticity*, Dover Publications, Inc., New York, 1996, p. 270.

[5] Kerschen, E. J., "Active Aerodynamic Control of Wake-Airfoil Interaction Noise–Theory," *Proceedings of the DGLR/AIAA 14th Aeroacoustics Conference*, Vol. 1, DGLR/AIAA Paper 92-02-039, Aachen, Germany, May 1992.

[6] von Kármán, T., and Burgers, J. M., "General Aerodynamic Theory—Perfect Fluids," *Aerodynamic Theory: A General Review of Progress*, edited by W. F. Durand, Vol. 2, Dover Publications, Inc., New York, 1963, pp. 304–310.

[7] Jaworski, J. W., and Gordnier, R. E., "High-Order Simulations of Low Reynolds Number Membrane Airfoils under Prescribed Motion," *Journal of Fluids and Structures*, Vol. 31, May 2012, pp. 49–66. doi: 10.1016/j.jfluidstructs.2012.04.003

A. Tumin
Associate Editor

Downloaded by MCGILL UNIVERSITY on March 20, 2013 | http://arc.aiaa.org | DOI: 10.2514/1.J051579